Magnetism of Nd^{3+} ions in $Nd_5Rh_4Sn_{10}$

S. Ramakrishnan and N. G. Patil
Tata Institute of Fundamental Research, Mumbai-400005, India

W. Kang and Heon Ick Ha
Ewha Women's University, Seoul 120-170, South Korea

Kim Yaung-Soo
Division of Joint Research Facility, Korean Basic Sciences, Durjeon, Korea

T. Takeuchi and Y. Miyako
Low Temperature Center, Osaka University, Toyanaka, Osaka 560-0043, Japan

A. A. Menovsky
Van der Waal-Zeeman Laboratorium, University of Amsterdam, Valckenierstrat, Amsterdam, The Netherlands

G. J. Nieuwenhuys and J. A. Mydosh
Kamerlingh Onnes Laboratory, Leiden University, Postbus 9504, 2300 RA Leiden, The Netherlands
(Received 24 October 2000; revised manuscript received 9 January 2001; published 30 March 2001)

In the family of rare-earth transition metal silicides, compounds belonging to the series $R_5Ir_4Si_{10}$ (where R is a rare-earth element from Dy to Lu and Y) exhibits multiple phase transitions. However, there exists a series $R_5Rh_4Sn_{10}$, which can only be formed with light rare-earth elements from Ce to Nd. In this work, we report detailed resistivity, susceptibility, magnetization, heat-capacity, thermal expansion, and magnetoresistance studies, which suggest that the Nd^{3+} moments undergo unusual magnetic orderings in a single crystal of $Nd_5Rh_4Sn_{10}$. A second-order magnetic transition at 7.15 K is followed by a first-order transition below 6.15 K that results in a huge heat-capacity peak of 100 J/mol K. The two transitions are strongly suppressed by a magnetic field (4 T) along the c axis while they are only weakly influenced by fields as high as 16 T in the basal plane. Moreover, the magnetoresistance data along the a and c axes from 1.5 to 15 K in fields up to 18 T revealed a giant positive magnetoresistance along the a axis below 6 K and clear evidence of a metamagnetic transition along the c axis. We attribute this unusual magnetic behavior to the unique crystal structure of this $Nd_5Rh_4Sn_{10}$ compound with its three different Nd sites.

DOI: 10.1103/PhysRevB.63.184402 PACS number(s): 74.70.Ad, 74.25.Bt, 74.25.Ha

Ternary rare-earth silicides and germanides of the type $Sc_5Co_4Si_{10}$ ($P4/mbm$) (Refs. 1 and 2) show the coexistence of magnetism or superconductivity with possible charge density wave ordering at high temperatures.[3,4] It turns out that in these compounds, the $3d$ atoms possess no magnetic moment. However, they participate in building up a high density of states at the Fermi level which is responsible for the superconductivity. One of the interesting features of this structure is the absence of direct transition-transition metal bonds. The transition metal atoms are connected to each other either through a rare-earth or Si atom. This is in marked contrast to the cluster-type superconducting compounds such as RMo_6S_8 and RRh_4B_4 which have been studied in great detail.[5] Earlier studies[6,7] showed that it was possible to form the $R_5Rh_4Sn_{10}$ (5410) series with light rare-earth elements. Recent studies in polycrystalline $Nd_5Rh_4Sn_{10}$ (Ref. 7) indicated an unusual magnetic ordering of Nd moments. Preliminary studies[8] on a crystal of $Nd_5Rh_4Sn_{10}$ reconfirmed the polycrystal data and suggested additional measurements. With a view to understanding the magnetism of Nd moments, we now report detailed resistivity, susceptibility, heat-capacity, thermal expansion, and high-field magnetoresistance behavior (1.5–15 K) along the a and c axes of a well-characterized single crystal of $Nd_5Rh_4Sn_{10}$.

A high-quality single-crystal sample has been synthesized using a Czochralski single-crystal apparatus described elsewhere.[9] Powder x-ray diffraction measurements showed that the sample $Nd_5Rh_4Sn_{10}$ has a tetragonal structure ($P4/mbm$) with no impurity phases. The lattice parameters a and c are found to be 13.912(1) Å and 4.591(1) Å, respectively. The single-crystalline nature of the sample was verified using the Laue diffraction technique. The crystal structure of this compound is illustrated in Fig. 1. $Nd_5Rh_4Sn_{10}$ adopts the $Sc_5Co_4Si_{10}$ ($P4/mbm$) type structure[1] where Nd atoms occupy three different sites of which Nd(1) has the highest local symmetry with its fourfold axis and the nearest Nd neighbor of Nd(1) lying along the c axis (4.591 Å). The two Nd(1) atoms are connected via short bonds to the Sn atoms and form a chainlike structure along the c axis. The Rh atoms separate the Nd(1) chains from the Nd(2) and Nd(3) atoms. The latter are connected to each other via short bonds and as a first approximation $Nd_5Rh_4Sn_{10}$ can be visualized as one-dimensional (1D) chains of Nd(1) atoms, which are embedded in a network of closely bonded Nd(2) and Nd(3) atoms.

The temperature dependence of the dc susceptibility (χ) and isothermal magnetization were measured using a com-

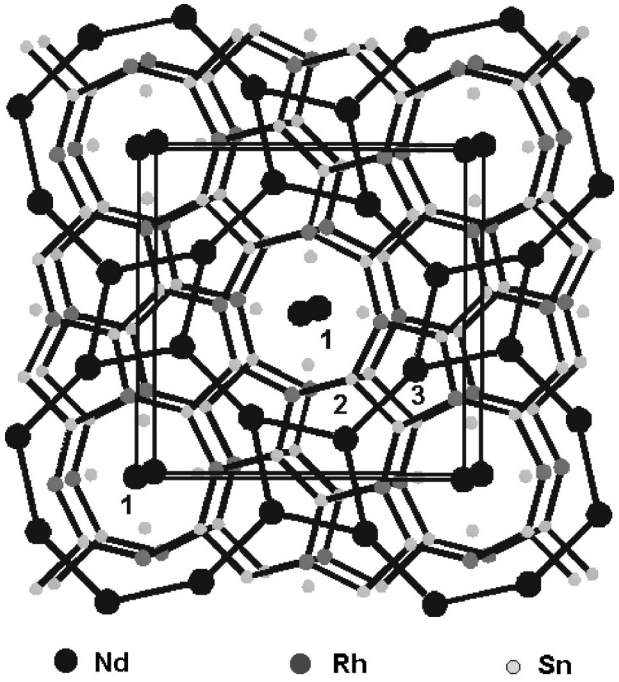

FIG. 1. Crystal structure of $Nd_5Rh_4Sn_{10}$ at 295 K. The Nd atoms have three inequivalent sites, which are marked 1, 2, and 3. The unit cell is also shown in the figure. Note that there is no direct Rh-Rh nearest-neighbor contact.

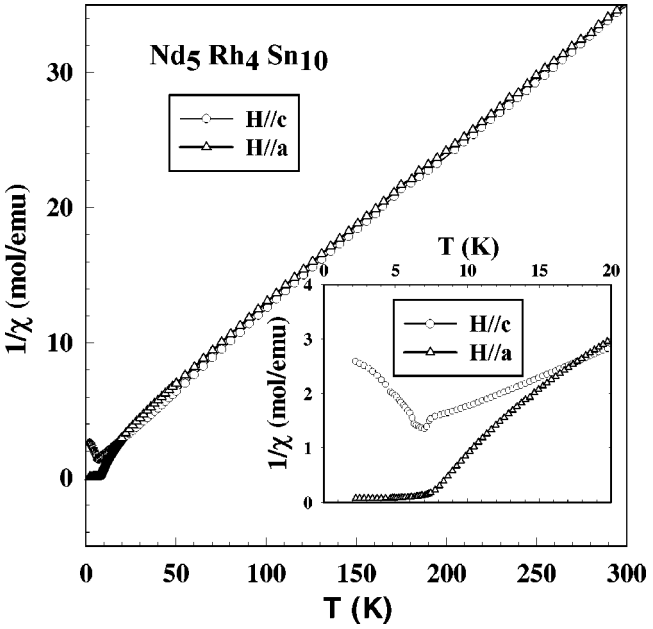

FIG. 2. Variation of the inverse susceptibility (χ^{-1}) of a single crystal of $Nd_5Rh_4Sn_{10}$ from 2 to 300 K. The inset shows the low-temperature χ^{-1} data with a slope change around 7.15 K along the *c* axis. There is an abrupt fall in $\chi(T)$ near 6.15 K, which probably suggests a first-order transition. Note that the transition along the *a* axis appears to be ferrimagnetic and there is no sharp fall at 6.15 K.

mercial superconducting quantum inferferrce device (SQUID) magnetometer (MPMS 5) from 2 to 300 K. The resistivity was measured using a four-probe dc technique with contacts made using silver paint on bar-shaped crystals of length 6 mm cut along the *a* and *c* axes. The temperature was measured using a calibrated Si diode (Lake Shore Inc.) sensor. The sample voltage was measured with a nanovoltmeter (model 182, Keithley) with a current of 5 mA provided by a current source (Hewlett Packard) with 20 ppm stability. All the data were collected using an IBM-compatible PC/AT via IEEE-488 interface. The relative accuracy of the resistance measurements is 50 ppm while the accuracy of the absolute resistivity is only 5% due to errors in estimating the geometrical factors. The heat capacity in zero field and in fields up to 10 T between 0.4 and 35 K was measured with an accuracy of 2% using an automated adiabatic heat pulse calorimeter using a ^{3}He Oxford cryostat. A calibrated RuO_2 resistance thermometer was used as the temperature sensor in this range. Magnetoresistance measurements were carried out in another high-field (18 T) Oxford ^{3}He system.

The temperature dependence of the inverse dc magnetic susceptibility (χ_{dc}^{-1}) of a crystal of $Nd_5Rh_4Sn_{10}$ along the *a* and *c* axes from 2 to 300 K is shown in Fig. 2. The low-temperature χ behavior along the respective axes is illustrated in the inset. The data along the *c* direction clearly show a peak at 7.15 K, which indicates the antiferromagnetic ordering of Nd^{3+} spins below this temperature. A sharp drop in susceptibility is observed at 6.15 K, which is followed by a gradual decrease in χ down to 2 K. In contrast, susceptibility along the *a* direction is large, further increases rapidly below 7.15 K, and finally shows a tendency to saturate at low temperatures. This can be ascribed to ferrimagnetic ordering in the *ab* plane. The magnetization data along the *a* and *c* directions support this view. Isothermal magnetization measurements along the *a* and *c* axes are shown in Fig. 3. The magnetization ($\mathbf{H}\|a$) is linear in **H** at 25 K, indicating the paramagnetic nature of the sample, while a nonlinear dependence of **M** on **H** beginning at 9 K implies the contributions of field-induced magnetic correlations above $T_1(=7.15\ \text{K})$. Note that a large residual ferromagnetic moment of $1.2\mu_B$ is already present at 6.8 K which increases to $2.2\mu_B$ at 5 K. However, the linear **M** vs **H** behavior ($\mathbf{H}\|c$) at 9 K indicates the presence of a paramagnetic state without any significant field-induced moments at this temperature. It must be said that the nonlinear behavior observed at 6.8 K agrees with the notion of antiferromagnetic ordering. Moreover, the **M** vs **H** data at 4.8 K show a slight upturn around 1.4 T which could be assigned to a weak metamagnetic transition which becomes fully developed at 3 T. Note that the **M**-**H** curve at 4.8 K intersects the **M**-**H** curves at 6.8 K and 9.8 K at 3.0 T and 2.8 T, respectively. The magnetization values decrease at lower temperatures, signifying that some of the spins are flipped away from the *c* axis below 6.15 K. To observe a metamagnetic transition at 3 K (similar to that at 4.8 K), one requires a field of more than 5 T. The magnetization data indicate that the Nd^{3+} spins align ferrimagnetically within the *ab* plane while an antiferromagnetic arrangement is favored along the *c* axis.

The high-temperature ($100\ \text{K} < T < 300\ \text{K}$) susceptibility along the *c* axis is fitted to a modified Curie-Weiss expression which is given by the relation

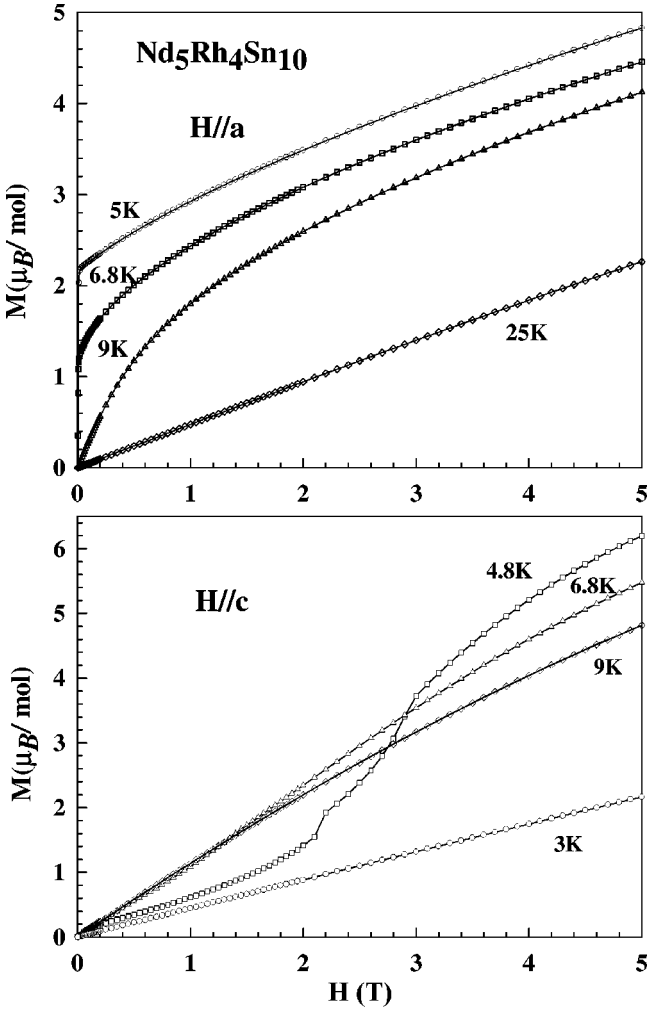

FIG. 3. Isothermal magnetization of a single crystal of $Nd_5Rh_4Sn_{10}$ at different temperatures. The usual linear **M** vs **H** plot at 25 K along the *a* axis above T_N suggests paramagnetism while it is strongly nonlinear at 9 K due to field-induced magnetism along the *a* axes (see also in Fig. 1 where χ data exhibit a large anisotropy below 15 K). The induced moment increases at low temperatures. However, there is no induced magnetism along the *c* axis. A metamagnetic transition along the *c* axis occurs at 4.8 K. Note that the magnetization decreases at 3.0 K along the *c* axis since the Nd spins are pulled away from the *c* axis towards the *ab* plane.

$$\chi = \chi_0 + \frac{C}{(T-\theta_p)}, \tag{1}$$

where C is the Curie constant which can be written in terms of the effective moment as

$$C(\text{emu/mol K}) = \frac{\mu_{eff}^2 x}{8}, \tag{2}$$

where x is the concentration of Nd ions ($x=5$ for $Nd_5Rh_4Sn_{10}$). The values of θ_p and μ_{eff} are found to be -15.4 K and $+3.9\mu_B$, respectively. Slightly lower values (-13.5 K and $+3.8\mu_B$) are obtained from a similar fit to the data along the *c* axis. The value of χ_0 is estimated to be about -1.6×10^{-4} emu/mol, which emphasizes the local moment nature of Nd^{3+} spins. The estimated effective moment of $3.9\mu_B$ is slightly higher than the free ion moment of the Nd^{3+} ion ($3.6\mu_B$). This suggests the contribution from conduction electrons of the Rh band to the effective moment. Below 100 K, the χ data show a deviation from the modified Curie-Weiss relation which could be due to the presence of crystal field contributions. It is rather surprising that there is almost no anisotropy in χ above 15 K, while it is considerable below this temperature. It could be accounted for by crystal field effects and the peculiar alignment of the Nd^{3+} spins below T_N which will be discussed later.

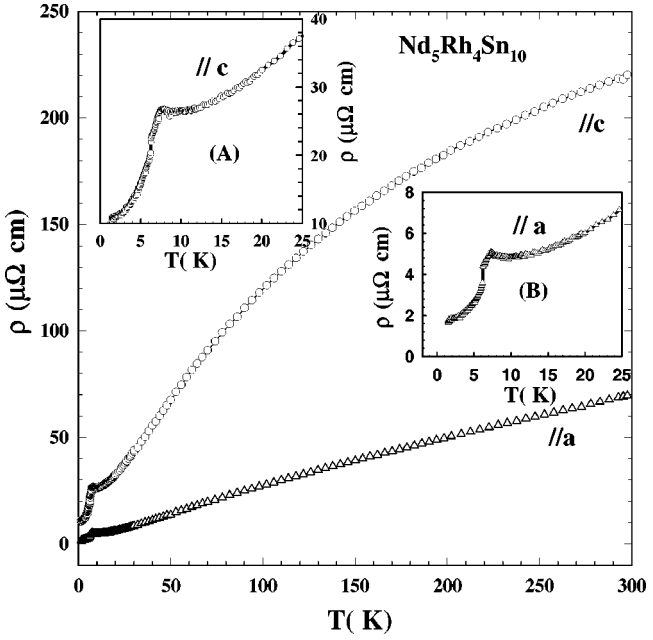

FIG. 4. Temperature dependence of the resistivity (ρ) of a single crystal of $Nd_5Rh_4Sn_{10}$ from 2 to 300 K. The inset shows the low-temperature ρ data from 2 to 30 K. A small kink in ρ near 7.15 K in the inset indicates antiferromagnetic ordering (T_N) in this compound. Note the sharp fall in $\rho(T)$ near 6.15K signifying a first-order transition (T_2).

The temperature dependence of the resistivity (ρ) of $Nd_5Rh_4Sn_{10}$ along the *a* and *c* axes is shown in Fig. 4. The insets show the low-temperature ρ data in an expanded scale. The ρ data show a change of slope at 7.15 K which is the antiferromagnetic ordering temperature (T_N) of this sample. This is in accordance with the T_N value obtained from the χ data. The resistivity along the *c* axis is 3 times larger than the resistivity along the *a* axis. This is in contrast to the absence of any anisotropy in $\chi(T)$ above T_N. In the temperature range (10 K$<T<$30 K), the temperature dependence of ρ could be fitted to the T^2 dependence which suggests that the spin fluctuations play a dominant role in scattering the conduction electrons. We also observe a shallow minimum in $\rho(T)$ around 10 K, which could possibly be ascribed to the presence of magnetic superzone effects. Such effects are also seen in pure Nd metal[10] as well as in $Dy_5Ir_4Si_{10}$ compound,[11] which is structurally similar to $Nd_5Rh_4Sn_{10}$. However, detailed neutron scattering measurements are needed to confirm this conjecture. The possibility of the Kondo effect as the cause for the resistivity minimum can be ruled out because

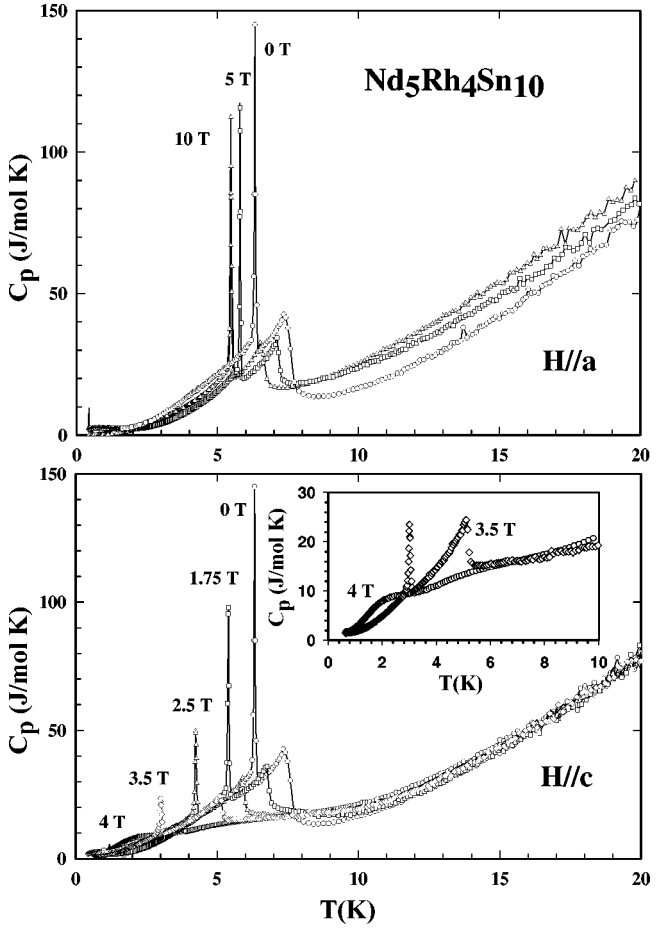

FIG. 5. Plot of C_p vs T of a single crystal of $Nd_5Rh_4Sn_{10}$ at various magnetic fields from 2 to 40 K for $\mathbf{H}\|a$ (upper panel) and $\mathbf{H}\|c$ (lower panel). The inset in the lower panel shows the same plot from 2 to 10 K for $\mathbf{H}=3.5$ and 4 T. A reasonable jump of 28 J/mol K at the first transition implies bulk magnetic ordering (T_N) of Nd^{3+} spins. However, the huge spike (100 J/mol K) at 6.15 K indicates that the lower transition (T_2) can only be ascribed to a first-order transition. The inset also displays the absence of magnetic transitions at 4 T in comparison with the two transitions observed at 3.5 T.

of the low χ_0 value and the absence of a minimum in ρ(T) when the antiferromagnetic transition is quenched above 4 T along the c axis. There is a sudden jump in the resistivity data below 6.15 K which is also present in the χ data along the c axis. We attribute this behavior in ρ to a first-order magnetic transition possibly involving an incommensurate-to-commensurate transition at 6.15 K. We have confirmed the first-order character by the observation of a small hysteresis in the ρ data via a cooling and warming cycle (not shown). Further, heat-capacity measurements (discussed below) also support this conclusion.

The temperature dependence of C_p from 0.4 to 20 K of $Nd_5Rh_4Sn_{10}$ at various applied magnetic fields along a and c axes is shown in Fig. 5. The inset gives the low-temperature C_p data for $\mathbf{H}=4$ T along the c axis. In the absence of a magnetic field, the C_p data show two large peaks at 7.15 K and 6.15 K, respectively. The first peak at 7.15 K ($\Delta C = 28$ J/mol K) unambiguously establishes the bulk magnetic ordering of the Nd^{3+} ions. But an even larger and sharper peak ($\Delta C = 100$ J/mol K) at 6.15 K shows evidence of first-order antiferromagnetic ordering in the absence of a structural transition (inferred from powder x-ray data at low temperatures) at this temperature. Heat-capacity measurements in magnetic field in both directions are also shown in Fig. Fig. 5. The data clearly show that both transitions have a strong field dependence in the c direction and vanish above a field of 4 T. In the ab plane C_p has a weak field dependence and exists for fields up to 10 T. The magnetic contribution to the heat capacity (which is obtained after subtracting the measured C_p data from that of $La_5Ir_4Sn_{10}$) suggests that the increase in the entropy at high temperatures ($T>15$ K) represents a contribution from crystal field effects. The total entropy below T_N is found to be 5 J/mol K, which is almost equal to the value of Rln2 and this indicates that the ground state is a doublet. Preliminary calculations support this view and the next excited state is also a doublet with a separation from this doublet ground state of approximately 50 K. Detailed calculations of the crystal field contribution to the heat capacity, susceptibility, and resistivity require a detailed model which will be published elsewhere. From the high-temperature heat-capacity data (10 K$<T<$25 K), we estimate the Debye temperature for this sample to be 300 K, and the γ value is of the order of 200 mJ/Nd mol K^2 which is very large and the reason for this large value could be attributed to the possible small splitting of the crystal field levels. However, detailed inelastic neutron scattering measurements are needed to confirm whether the crystal field states indeed contribute to this large γ value.

Figure 6 illustrates the thermal expansion ($\Delta l_i/l_i$) data along the a and c axes from 5 to 300 K. The two insets show the same data, which elucidate the two antiferromagnetic transitions. We define the thermal expansion as

$$\Delta l_i/l_i = [l_i(T) - l_i(4.5\ \text{K})]/l_i(4.5). \tag{3}$$

The upper and lower insets show the low-temperature data along the a and c axes, respectively. The thermal expansion is nearly linear in a temperature down to 100 K and deviates from linearity below this temperature. $\Delta l_a/l_a$ is always positive and continues to decrease towards zero down to 4.5 K, whereas $\Delta l_c/l_c$ becomes negative below 70 K and increases slowly towards zero at 4.5 K. The arrows marked in the upper and lower insets indicate changes in $\Delta l_a/l_a$ and $\Delta l_c/l_c$ values, which signify the observed magnetic transitions. Figure 7 displays the temperature dependence of the thermal expansion coefficient $[\alpha = d(\Delta l/l)/dT]$ from 4.5 to 100 K. The upper and lower insets show the low-temperature data spanning the phase transitions along the a and c axes, respectively. The sharp anomaly at 6.15 K and the broad anomaly at 7.15 K clearly portray the first- and second-order natures of the magnetic transitions. The temperature dependence of α_a is quite similar to the observed anomaly in the heat capacity.

Figure 8 shows the field dependence of the resistivity $[\rho(\mathbf{H})]$ along the c axis at different temperatures of a single

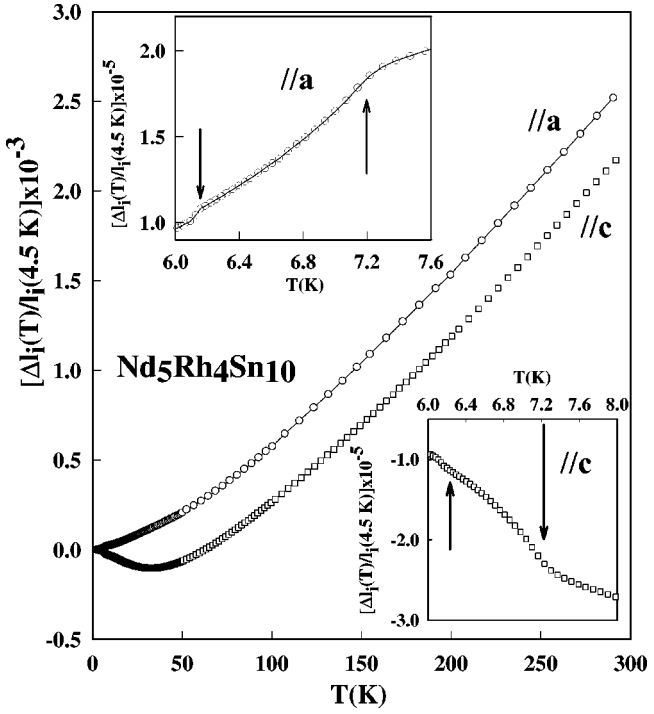

FIG. 6. Plot of the thermal expansion data of a single crystal of $Nd_5Rh_4Sn_{10}$ along the *a* and *c* axes from 4.5 to 300 K. The upper and lower insets show the low-temperature data along the *a* and *c* axes, respectively. The arrows indicate the first-order spin reorientation transition at T_2 and a second-order antiferromagnetic transition at T_N.

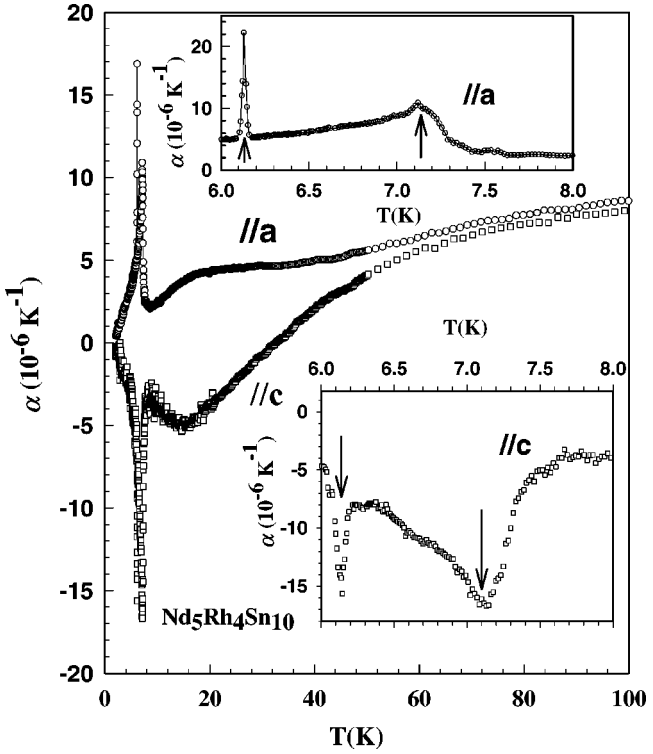

FIG. 7. The thermal expansion coefficient of a single crystal of $Nd_5Rh_4Sn_{10}$ along the *a* and *c* axes from 4.5 to 300 K. The upper and lower insets show the low-temperature data along the *a* and *c* axes, respectively. The data along the *a* axis are a replica of the one obtained via heat-capacity studies. The broad anomaly at 7.15 K and the sharp peak at 6.15 K indicate the magnetic transitions (indicated by the arrows) have second- (T_N) and first-order (T_2) characteristics at these temperatures.

crystal of $Nd_5Rh_4Sn_{10}$ from 1.5 K to 15 K. It can be clearly seen that the magnetoresistance decreases by 25% at 10 T for $T=15$ K which is well above the ordering temperature of 7.15 K. Moreover, the transition at 7.15 K is antiferromagnetic in nature which is expected to exhibit a positive magnetoresistance. The negative magnetoresistance above T_N reflects the reduction of spin disorder scattering due to field alignment of the moments in the paramagnetic state. The reduction in $\rho(\mathbf{H})$ progressively increases and reaches nearly 50% at 10 T for $T=8$ K. However, for $T\leqslant 6.15$ K, there is an abrupt jump in $\rho(\mathbf{H})$ and the field at which the step occurs increases as the temperature [where $\rho(\mathbf{H})$ is measured] decreases. We attribute this jump to the occurrence of a metamagnetic transition along the *c* axis (see also Fig. 3). After the jump, $\rho(\mathbf{H})$ starts to increase as a function of field in contrast to its behavior for $T>6.15$ K. In addition, the functional dependence [$\rho(\mathbf{H})$ vs $\mathbf{H}$] for $T<6.15$ K is different from that of $\rho(\mathbf{H})$ for $T>6.15$ K. All of the above observations are consistent with occurrence of a metamagnetic transition beginning around 2.5 T along the *c* axis below 6.15 K. We wish to point out that the magnetoresistance data clearly display a metamagnetic transition below 6.15 K as compared to the magnetization data shown in Fig. 3. The jump in ρ observed at 3.2 T for $T=1.4$ K rapidly moves down to 0.7 T at $T=6.0$ K.

The field dependence of resistivity $\rho(\mathbf{H})$ along the *a* axis at different temperatures for a crystal of the same batch from 1.5 K to 15 K is also shown in Fig. 7. At $T=15$ K, $\rho(\mathbf{H})$ along the *a* axis weakly depends on the field unlike the $\rho(\mathbf{H})$ along the *c* axis. However, below 6 K, $\rho(\mathbf{H})$ (positive magnetoresistance) increases rapidly with field, reaching 200% $[\rho(\mathbf{B})-\rho(0)]/\rho(0)$ at 3 T and about 300% at 10 T for $T=1.5$ K. The functional dependence of $\rho(\mathbf{H})$ below 6 K has also changed similar to that along the *c* axis. It is interesting to note that the magnetoresistance data at $T=6.0$ K exhibit a small hysteresis which is absent in all other ($\mathbf{H}\|a,\mathbf{I}\|a$) data. This could be ascribed to the fact that the spin flip occurs close to this temperature and that could cause the observed hysteresis. Finally, the $\rho(\mathbf{H})$ values at different temperatures tend to reach a common value at fields higher than 17 T. This is attributed to the fact that the magnetization energy at 17 T becomes comparable to the thermal energy at these temperatures.

Our measurements using a single crystal of $Nd_5Rh_4Sn_{10}$ suggest that the Nd moments order antiferromagnetically along the *c* axis while a ferrimagnetic ordering is observed in the *ab* plane in an applied field of 1 T. The observation of a positive magnetoresistance for $T\leqslant 6.2$ K along the *c* axis up to the field at which the metamagnetic transition occurs is consistent with the above scenario. However, the $\rho(\mathbf{H})$ for $T\leqslant 6.2$ K is also positive along the *a* axis which is not in agreement with the notion of ferrimagnetism in the *ab* plane. Generally, in compounds that exhibit metamagnetism, one

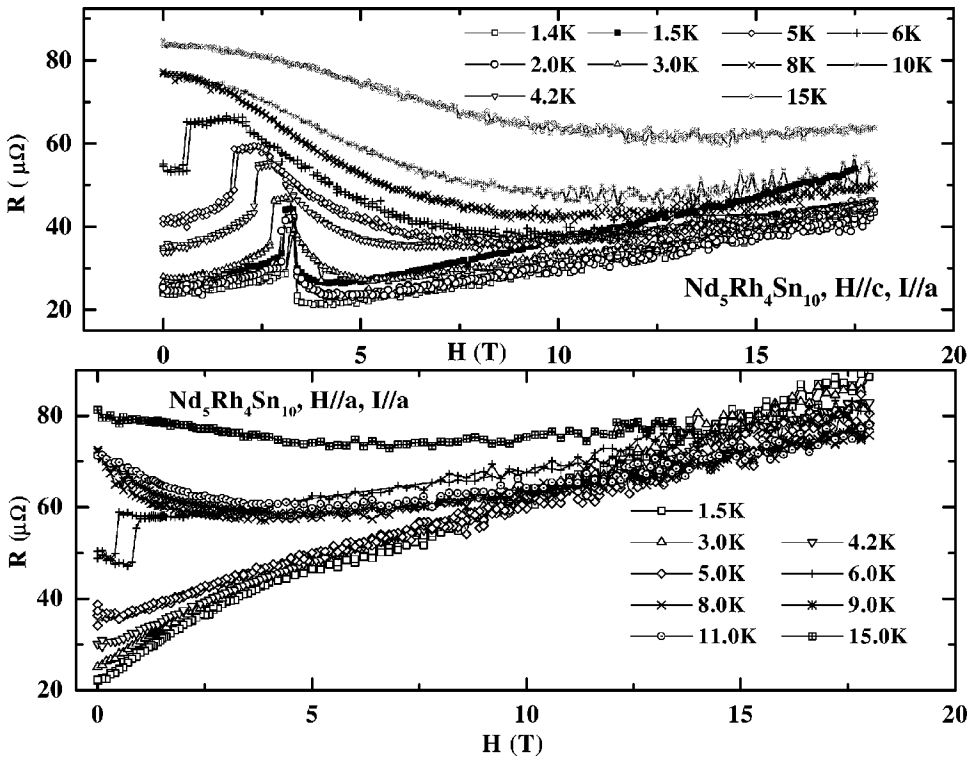

FIG. 8. The magnetoresistance $[\rho(\mathbf{H})]$ of $Nd_5Rh_4Sn_{10}$ from 0 to 18 T at different temperatures along *c* (upper panel) and *a* (lower panel) axes. Large positive magnetoresistance is observed along the *a* and *c* axes and it changes to negative magnetoresistance at higher temperatures ($T>8$ K). Note that the sharp peak corresponds to the metamagnetic transition along the *c* axis.

expects a maximum in $\rho(\mathbf{H})$ followed by a drop at a critical field $\mathbf{H}_c$. This is because in a Néel model with two sublattices, the dominating effect is the loss of periodicity due to a reversal of moments residing in the sublattice with antiparallel orientation.[12] A similar increase of $\rho(\mathbf{H})$ up to the metamagnetic transition is also expected for band antiferromagnets.[13] Although a maximum in $\rho(\mathbf{H})$ is observed in $Nd_5Rh_4Sn_{10}$, we also note the subsequent increase in $\rho(\mathbf{H})$ in both directions at higher fields. Neutron scattering measurements at high fields are required to solve this issue. In any case, the magnetoresistance data vividly demonstrate that the high magnetoresistance [giant magnetoresistance (GMR)] is due to the anisotropy and unusual spin arrangements in $Nd_5Rh_4Sn_{10}$.

Our preliminary neutron scattering data indicate that the moments at the Nd(1) site (0,0,0) order antiferromagnetically in the *c* direction while the eight spins at other sites, Nd(2) (0.18,0.68,0.5) and Nd(3) (0.39,0.89,0.5), order ferrimagnetically within the *ab* plane. Below 6.15 K, the Nd(1) spin flips in the direction of the *ab* plane in an alternating manner. This causes the magnetic unit cell to double in the *a* and *b* directions, which is accompanied by a first-order transition with a huge heat-capacity jump of 100 J/mol K. To explain the field dependence of the heat-capacity data, we propose a model in which the Nd^{3+} moments strongly align ferrimagnetically within the *ab* plane but this plane is antiferromagnetically coupled to the next plane along the *c* axis. Such an alternate coupling is very weak but capable of inducing a moment reorientation at 6.15 K. However, this weak coupling along the *c* axis is extremely susceptible to the applied field and it can be completely suppressed for fields above 4 T. A transition of this kind is quite novel in the study of magnetic ordering in various rare-earth systems. We caution that the above-mentioned simple scenario is only one plausible explanation to account for the various bulk properties observed in $Nd_5Rh_4Sn_{10}$. To understand the suppression of the transition with field along *c* axis and to explain the observed giant magnetoresistance (positive below $T<15$ K along both the *a* and *c* axes, and negative for $T>6.15$ K along the *c* axis), one requires detailed neutron scattering measurements on a single crystal both with and without an applied magnetic field.[14]

In summary, we conclude that the Nd^{3+} moments in light rare-earth $Nd_5Rh_4Sn_{10}$ exhibit unusual ordering due to the unique 5-4-10 structure with three different Nd sites. It was shown that the heavy rare-earth compounds of the same structure ($R_5Ir_4Si_{10}$) (Refs. 3 and 4) display the coexistence of charge-density-wave (CDW) ordering with superconductivity or magnetism. Although there is no CDW ordering in $Nd_5Rh_4Sn_{10}$ (due to its large volume as compared to that of heavier rare earths), the occurrence of the sharp first-order transition and the giant positive magnetoresistance is primarily due to the above-mentioned ordering of the Nd^{3+} moments.

[1] H.F. Braun, J. Less-Common Met. **100**, 105 (1984).
[2] S. Ramakrishnan and K. Ghosh, Physica B **223&224**, 154 (1996).
[3] B. Becker, N.G. Patil, S. Ramakrishnan, A.A. Menovsky, G.J. Nieuwenhuys, J. Mydosh, M. Kohgi, and K. Iwasa, Phys. Rev. B **59**, 7266 (1999).
[4] F. Galli, S. Ramakrishnan, T. Taniguchi, G.J. Nieuwenhuys, J.A. Mydosh, S. Geupel, J. Lüdecke, and S. van Smaalen, Phys. Rev. Lett. **85**, 158 (2000).
[5] O. Fisher, in *Magnetic Superconductors*, edited by K. H. J. Buschow and E. P. Wohlfarth (Elsevier, Amsterdam, 1990), Chap. 6.
[6] G. Venturini, B. Malaman, and B. Roques, Mater. Res. Bull. **24**, 1135 (1989).
[7] N.G. Patil and S. Ramakrishnan, Phys. Rev. B **56**, 3360 (1997).
[8] N.G. Patil and S. Ramakrishnan, J. Appl. Phys. **85**, 4845 (1999).
[9] A.A. Menovsky and J.J.M. Franse, J. Cryst. Growth **65**, 286 (1983).
[10] Review by S. Levgold, in *Magnetic Properties of Rare-Earth Metals*, edited by R. J. Elliot (Plenum, New York, 1972), p. 335.
[11] S. Ramakrishnan, K. Ghosh, and Girish Chandra, Phys. Rev. B **45**, 10 769 (1992).
[12] H. Yamada and S. Takada, J. Phys. Soc. Jpn. **34**, 51 (1973).
[13] K. Usami, J. Phys. Soc. Jpn. **45**, 466 (1978).
[14] N. G. Patil (private communication).